JOURNAL OF Materials CHEMISTRY

Macroporous silica and titania obtained using poly[styrene-*co*-(2-hydroxyethyl methacrylate)] as template

María C. Carbajo,[a] Adrián Gómez,[b] María J. Torralvo*[a] and Eduardo Enciso[c]

[a]*Departamento de Química Inorgánica I, Universidad Complutense de Madrid, 28040 Madrid, Spain*
[b]*Centro de Microscopía Electrónica, Universidad Complutense de Madrid, 28040 Madrid, Spain*
[c]*Departamento de Química-Física I, Facultad de Ciencias Químicas, Universidad Complutense de Madrid, 28040 Madrid, Spain*

Received 2nd January 2002, Accepted 10th June 2002
First published as an Advance Article on the web 30th July 2002

Ordered macroporous silica and titania have been prepared using poly[styrene-*co*-(2-hydroxyethyl methacrylate)] (PS-HEMA) latex arrays as templates. Polystyrene (PS) particles have also been used to template macroporous titania. Arrays of spherical latex particles, with average diameters of 260 nm (PS-HEMA) and 390 nm (PS), have been obtained by either evaporation of the solvent at room temperature or by deposition on filtration membranes. In both cases, 3D extended regions with cubic close packing of microspheres are observed, but in the samples obtained after evaporation of the solvent the self-assembled particles show a higher degree of order. The oxides were synthesized by hydrolysis of sodium silicate or titanium isopropoxide (diluted in *n*-propanol or hexane) which were infused into the cavities of the latex arrays. Two different methods have been used to fill the cavities with the precursor: filtration with suction and capillary forces. When solidification of the ceramic matrix took place, the template was eliminated by heating at 500 °C. As replica of the latex assemblies, periodic porous silica and titania were obtained. Sheets of amorphous silica, as thin as 4–7 nm, form the wall of the interconnected pores whose diameters range from 200 to 220 nm. In macroporous titania obtained from titanium isopropoxide diluted in *n*-propanol and imprinted on PS-HEMA particles, the pore diameters range from 160–180 nm. The porous network is shaped by walls that are 8–12 nm thick and are formed from anatase nanocrystals with a major dimension of 8–20 nm. Pore diameters, crystallite sizes and thicknesses are similar when hexane is used as the solvent of the inorganic precursor. However, in macroporous titania imprinted on PS particles, nanocrystals with a major dimension of 6–10 nm form the pore wall with a thickness of 6 to 8 nm. Interactions between the titania precursor and the latex particles seem to affect the microstructural parameters. The porous skeleton of titania is preserved after treatment at 600 °C for 16 hours but the pore wall thickness slightly increases with crystallite growth and in some particles disordered areas appear.

Introduction

The synthesis of periodic porous solids with tailored pore size is a current challenge for fundamental research and also because such long-range ordered porous materials have potential in a variety of applications.[1–3] In the last few years templating methods have proved successful for the design of hierarchical porosity[4–6] as the size of the templating beads could be modified. Surfactant arrays[4,7] and emulsion droplets[8,9] or particles[5,10–13] have been used as templates and a wide range of structured porous materials have been prepared including inorganic oxides,[10,12,14,15,17] carbons,[11] metals,[16] and polymers.[18]

Monodisperse latex microspheres of controlled size and variable composition can be produced and three-dimensionally ordered arrays of particles can be obtained in accurately controlled conditions.[19–21] Therefore, arrangements formed by latex microspheres have been extensively used as a target on which to template advanced materials. The microspheres are assembled into ordered arrays by filtration, sedimentation or centrifugation, and the way in which the cavities between the particles are mineralized includes a variety of infusing routes, such as sol–gel hydrolysis, polymerization, electrochemical deposition or precipitation.[6,22] The assembling of the latex usually results in microdomains with different orientations because nucleation and growth are affected by the concentration of the dispersion, the interparticle interactions and kinetic factors, which operate when the solvent is eliminated.[6,19] The creation of continuous ordered networks adequate for fabrication of useful devices requires control of the assembly process and the infusing routes leading to the mineralization of interparticle spaces. Therefore, much work must be done in this field in order to understand the driving interparticle interactions in the template and also the interaction between the target and the precursor of the porous structures.

In this work we describe our results on the synthesis of macroporous silica and titania templated by PS-HEMA latex microspheres. This latex has been selected because the particles easily form highly ordered films.[23] Therefore, it could be used advantageously to prepare ordered porous solids, although we are not aware of the use of this latex as a template. Self-assembly behaviour of these latex particles after the solvent has been removed by filtration and by evaporation has been compared. Moreover, since the chemical properties of a particle's surface must affect the condensation of the inorganic precursor that produces the solid matrix, the influence of the surface of the HEMA chains on the mineralization process has also been investigated. PS latex particles have also been used to

 DOI: 10.1039/b200047b

template macroporous titania and the results obtained from both kinds of latex have been compared.

Experimental

Synthesis of latex microspheres

Poly[styrene-*co*-(2-hydroxyethyl methacrylate)] (PS-HEMA) and polystyrene (PS) were prepared by emulsion copolymerization of styrene (S) and 2-hydroxyethyl methacrylate (HEMA),[23] and emulsion polymerization of styrene[24] respectively. Reagent grade materials from Sigma and distilled water were used in the experiments. The polymerization was carried out in a 250 cm^3 round-bottomed five-necked flask equipped with a glass stirrer with a PTFE paddle, thermometer and a gas inlet providing a constant flow of nitrogen gas. A water-cooled reflux condenser was inserted into the other outlet. Initially water was added to the flask, together with the monomers (215 ml of water and 1.4 mol l^{-1} of styrene in the synthesis of PS and 215 ml of water, 1.4 mol l^{-1} of styrene and 0.16 mol l^{-1} of HEMA in the synthesis of PS-HEMA). After 15 minutes of N_2 purging and stirring the mixture, the initiator (0.002 mol l^{-1} of potassium persulfate) was added to the reactor flask. The polymerization was carried out at 70 °C for 10 hours with a constant stirring speed of 350 rpm. The reaction flask was maintained at the required constant temperature ($\pm$ 2 °C) by using a thermostatic water bath. In each case, the resulting latex was filtered through glass wool into well-washed dialysis tubing (a membrane from Sigma) and then, dialysed for four weeks against water.

Preparation of latex arrays

Samples of dialysed PS-HEMA and PS latex were taken from the water-based dispersions and were used to prepare the latex arrangements by: i) evaporation of the solvent and ii) deposition on filtration membranes.

i) Evaporation of the solvent. Samples from the original dispersions with a concentration of 7.43% (w/w) for PS-HEMA and 2.17% (w/w) for PS were dried at room temperature under air and then kept over a desiccant for 24–72 hours.

ii) Deposition on filtration membranes. In this case the original dispersions were diluted to a final concentration of 0.1% (w/w) for PS-HEMA and 0.05% (w/w) for PS and filtered under atmospheric pressure, using Millipore membranes with pore diameter of 0.2 μm. In order to estimate the variation of the concentration during the filtration process, small volumes of dispersion were taken from the filtration vessel from time to time and the UV/Vis spectrum of every aliquot was recorded. The intensity of the absorbance maximum (at $\sim$235 nm) corresponding to phenyl groups was compared in the series of spectra. The deposited latex layers were dried over a desiccant for 24–72 hours.

Preparation of macroporous structures

Thick dry latex films without previous thermal treatment were used as templates to prepare macroporous SiO_2 and TiO_2. The oxides were obtained from solutions containing the inorganic precursors, which were confined inside the free space between the latex microspheres. As precursors sodium silicate and titanium isopropoxide solutions were used, respectively (in both cases reagent grade from Sigma). To ensure that spaces between spheres were filled by the solution before polymerization of the precursor, the concentration and pH value of the sodium silicate solution were adjusted to allow adequate gelation time. Titanium isopropoxide was diluted in *n*-propanol (weight ratio alkoxide : alcohol $\approx$ 0.6) or hexane (weight ratio alkoxide : hexane $\approx$ 0.2), to prevent premature reaction. The precursor solutions were introduced into the cavities of the latex arrays by two different methods: filtration with suction or using capillary forces. In the first case, the solution of the precursor was added dropwise to cover pieces of the latex arrays of millimetre size placed on a filtration membrane and suction was applied for 2–3 minutes. In the second case the edge of the latex films were placed in contact with the solution to allow the latter to enter into the arrays. In each case, after 2–3 hours, the composite solids were placed over a desiccant for 24–72 hours. Then, the solids were treated at 500 °C in air for 3 hours. A titania sample was also treated at 550 °C and 600 °C for 16 hours.

Characterization

Latex dispersions. The diffusion constant of freely moving particles in the dispersions was measured by photon correlation spectroscopy (quasi-elastic light scattering, QELS). The hydrodynamic diameter of the particles was obtained from the diffusion constant by the Stokes–Einstein equation. A focused beam of an argon laser (coherent CR9D-3, λ = 514.4 nm) was directed into a temperature-stabilized (25 °C) cylindrical cell. The scattered light was collected by the receiving optics at a 90° angle. The photon counts of the photomultiplier (EWMI 9863) were processed by a digital correlator (ALV-3000) linked to a computer. Data analysis was based on a second-order cumulant fit procedure. In addition, the second cumulant normalized to the square of the first cumulant was determined to provide some information on the width of the particle size distribution.

2D and 3D structures. The latex arrays and the inorganic macroporous oxides have been characterized by scanning electron microscopy (SEM) and transmission electron microscopy (TEM). TEM was also used to characterize the morphology and mean diameter of the latex particles. The samples for SEM were coated with a gold film before observation in a JEOL-6400 electron microscope working at 20 kV. Transmission electron micrographs and electron diffraction patterns were taken with a JEOL 2000FX electron microscope operating at 200 kV and equipped with a double tilting ($\pm$45°) sample holder. The samples for TEM were prepared as follows: the samples of latex were taken from the original suspension and diluted with water to a concentration of about 1% (w/w). Drops of these dispersions were placed on 3 mm Cu grids coated with holey carbon support films. In the case of SiO_2 and TiO_2, the samples were prepared by ultrasonic dispersion in *n*-butanol and by depositing drops of the dispersion over the copper grids.

Results and discussion

Latex particles behaviour

The spherical particles of PS-HEMA and PS (Fig. 1) are monodisperse with a diameter of about 260 nm (PS-HEMA) and 390 nm (PS). These values are about 13% lower than the hydrodynamic diameter as obtained by QELS. The differences can be attributed to the fact that in the dispersion the moving charged particles carry part of the adsorbed layer, and in the case of PS-HEMA, also to the hydrophilic swelling surfaces, as has been suggested previously.[23] The images in Fig. 1a–c show a high degree of ordering in the 2D and 3D arrays of PS-HEMA. In Fig. 1c we can distinguish face centered cubic (fcc) packing of particles projected along a direction close to [111]. Roughness and contrast changes are observed on the surface of PS-HEMA microspheres (Fig. 1b), whereas PS particles have polished surfaces (Fig. 1d, 1e). Images in Fig. 1b (PS-HEMA) and Fig. 1e (PS) show interparticle necks formed in the outer shell at particle–particle contact areas.

The top surface of pieces of PS-HEMA layers in the

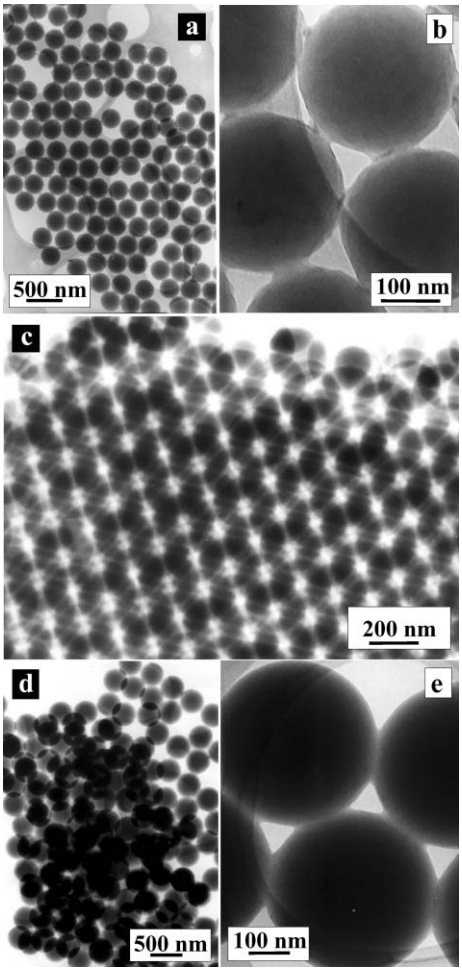

Fig. 1 TEM micrograhs showing 2D (a,b,e) and 3D (c,d) arrays of ordered PS-HEMA particles (a–c) and PS particles (d,e).

millimetre-size range shows extensive regions with 2D close packing together with a few defects (Fig. 2a). The ordering extends over three dimensions as suggested by the fracture surface in Fig. 2b. Highly ordered arrays of PS particles are also observed, but in this case more defects appear (Fig. 2c). When the samples of both PS-HEMA and PS are obtained by deposition on filtration membranes a microstructure in domains is frequently obtained (Fig. 3). The top surface of a thick film of PS-HEMA shows areas with hexagonal packing which coexist with square packing, other kinds of packing and disordered regions (Fig. 3a). The deposited films have almost uniform thickness (Fig. 3b and the enlarged view in Fig. 3c) which range from about 10 μm to 100 μm.

The formation of latex particle assemblies has been extensively investigated.[19,25–27] It is known that within the liquid dispersion, monosized highly charged latex particles could spontaneously organize themselves into different structures. These ordered configurations are stabilized by electrostatic repulsion, which keep the particles apart at distances larger than the particle diameter.[19,21] Both, the chemical nature of the latex surface and the conditions in which the solvent is eliminated affect the kind and efficiency of packing.[19,21,28] Denkov *et al.*[27] have observed by optical microscopy the dynamics of 2D crystallization from aqueous dispersions of latex particles and they have shown that nucleation and crystal growth occur by attractive capillary forces and convective particles flux during evaporation of the water. Self-assembled PS-HEMA particles produce highly ordered arrays and, this fact has been related to the poly-HEMA segments at the surface of the particles.[23] It has been suggested that in the PS-HEMA latex, the poly-HEMA chains assist the ordering,

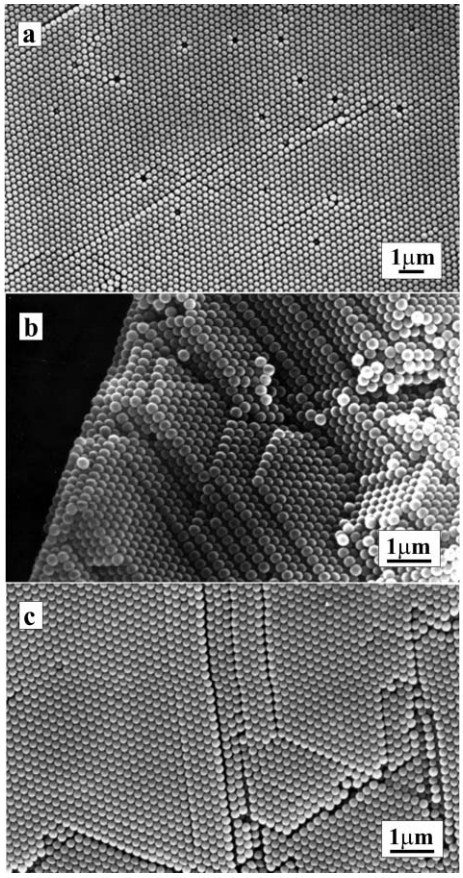

Fig. 2 SEM micrographs showing top surfaces (a,c) and fracture surface (b) of PS-HEMA (a,b) and PS (c) latex films obtained by evaporation of the solvent.

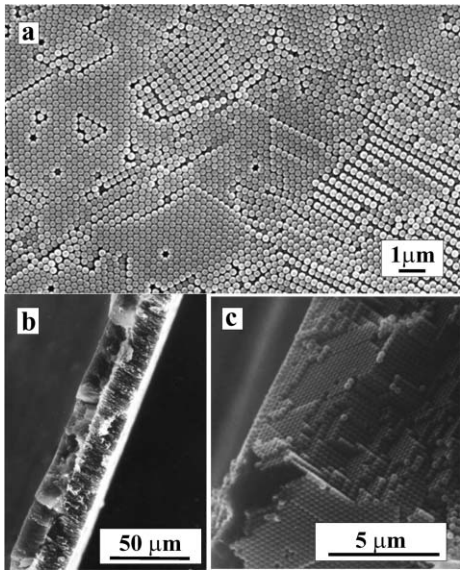

Fig. 3 SEM micrographs of a PS-HEMA film obtained by deposition on a filtration membrane. Top surface (a), fracture surface (c) and thickness (b) are shown.

since the chains at the surface of the particles constitute a hydrophilic swollen shell which contracts when the solvent is removed and the particles are pulled together, provided that the capillary forces progressively increase.[23] Our TEM and SEM observations agree well with these ideas. Both, PS-HEMA and PS particles could organize themselves in an ordered way by evaporation of the solvent (Fig. 2). Even in dilute dispersions, where the latex volume fraction is about 1%, the flux of

PS-HEMA particles governed by capillary forces produces ordered configurations (Fig. 1a and c). The fact that interparticle necks are formed when the water is removed (Fig. 1e) indicates the viscoelastic character of the latex surface due to the low glass temperature (T_g) of these latexes.

In the case of assemblies attained by a filtration process, the water is eliminated under pressure and the particles deposited on the surface by convective forces.[29] The UV/Vis spectra of aliquots taken from the dispersion during the filtration experiments show an absorption band with a maximum at $\sim$235 nm, which corresponds to aromatic groups. The lack of significant changes in the intensity of this band during deposition indicates that no significant variations in the concentration of the dispersion occur during the process. In this way the filtration speed actually represents the speed of the particles arriving at the surface. Therefore, the kinetics of the process, cooperative effects and steric factors must affect nucleation and array growth and they must determine the assembly behaviour of the particles. Nevertheless, deposition by filtration is a simple method and the degree of order that can be attained can be good enough for many practical applications.

Inorganic porous structures

Macroporous silica and titania imprinted on PS-HEMA microspheres. The precursor solutions of silica and titania (titanium isopropoxide diluted in *n*-propanol) were infused by filtration with suction into the latex films, which were previously assembled by evaporation of the water at room temperature. The elimination of the template during treatment of the composite materials at 500 °C produces inorganic matrices with ordered porous structure. The extended view of the top surface of the particles for SiO_2 and TiO_2 (Fig. 4), shows microstructures in which ordered domain up to about 10 μm in size are separated by defective boundaries (Fig. 4c). The micrographs show together with the porosity replica of the latex microspheres, a sublattice of smaller pores at a position corresponding to the interstices between the template particles. In the TEM images (Figs. 5 and 6) the networks of three-dimensionally interconnected pores (clearer areas) in the framework of silica and titania (darker areas) can be observed. Micrograhs (a), (b) and (c) in Fig. 5 show the same flake from a ground sample of amorphous silica and (d) and (e) show another particle from the same sample. The Fourier's transforms of the images are shown in the insets. The patterns show high intensity spots, which can be indexed in a fcc lattice along the [100], [110], [211] and [111] directions respectively. The projection along the [111] direction (Fig. 5d and e) reveals the skeleton of silica formed by filling the tetrahedral and octahedral holes of the porous network and the thickness of the ceramic building the pore walls. The windows interconnecting the pores are partially closed by a thin shell of silica as the changes in the contrast in the clear areas of the images reveal. The pore diameter ranges from 200 to 220 nm as estimated from the images corresponding to the projection along the (100), (110) and (111) planes. From the projection along the [111] direction the wall thickness was also estimated. The values obtained range from 4 to 7 nm. In the porous skeleton the mean distance between pore centres was measured and the value was compared with the sphere centre-to-centre mean distance in the templating arrays. The difference between the two values indicate that shrinkage of the structure by about 22% occurs during infusion of the ceramic precursor and the thermal treatment.

The porous networks of macroporous titania (Fig. 6) is supported by a framework of anatase nanocrystals (see the inset in Fig. 6a). This image corresponds to a particle oriented close to the [110] direction and shows the pore walls formed of nanocrystals with a major dimension of 8–20 nm. In this

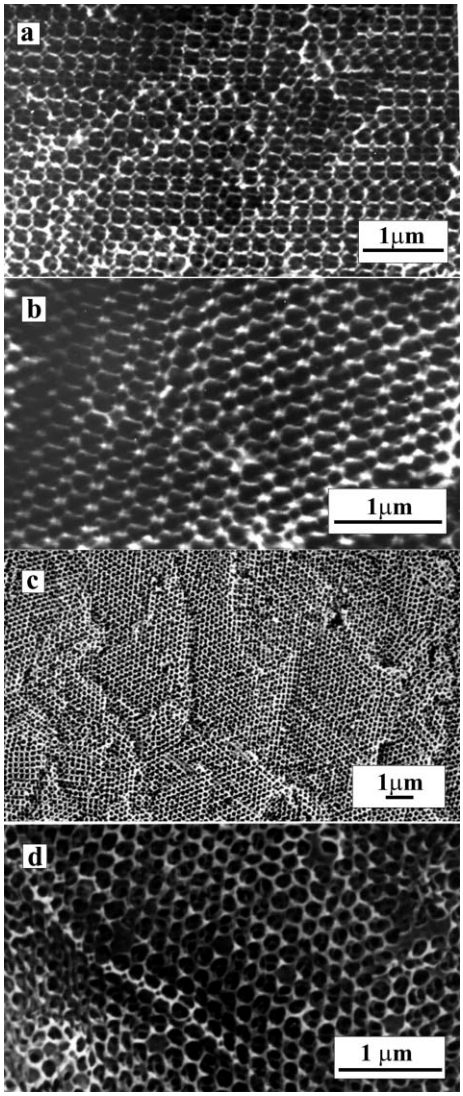

Fig. 4 SEM micrographs of macroporus SiO_2 (a–c) and TiO_2 (d) imprinted on PS-HEMA and treated at 500 °C for 3 hours.

sample the pore diameters range from 160 to 180 nm as estimated from the projection along the [110], [111] (Fig. 6b and c) and [100] (not shown) directions. Care must be taken when the pore wall thickness is estimated from the images, since higher values than the actual value can be obtained with thick particles in which the pore wall of consecutive pore layers could be not entirely superposed. Values ranging from 8 to 12 nm were obtained using thin flakes from the sample projected along the [111] directions (Fig. 6c). The contraction of the structure is about 30% as estimated from the distances between the pore centres.

Macroporous titania was also obtained using titanium isopropoxide diluted in hexane (weight ratio $\approx$ 0.2) as precursor. In this case PS-HEMA microspheres were assembled by deposition on filtration membranes and the cavities were filled with the precursor solution using capillary forces. A well ordered porous structure can be observed in most of the particles of this sample (Fig. 7a and Fig. 7b), although in some of them regions of disorder appear. The values of the mean pore diameters (160–175 nm), pore wall thicknesses (8–15 nm) and crystallite sizes (major dimension of 10–15 nm) are similar to those obtained when *n*-propanol is used as the solvent of the precursor.

In these porous solids, the structure of the pore walls and the wall thickness depend on the viscosity of the precursor solution and the hydrolysis and condensation rates. In the case of

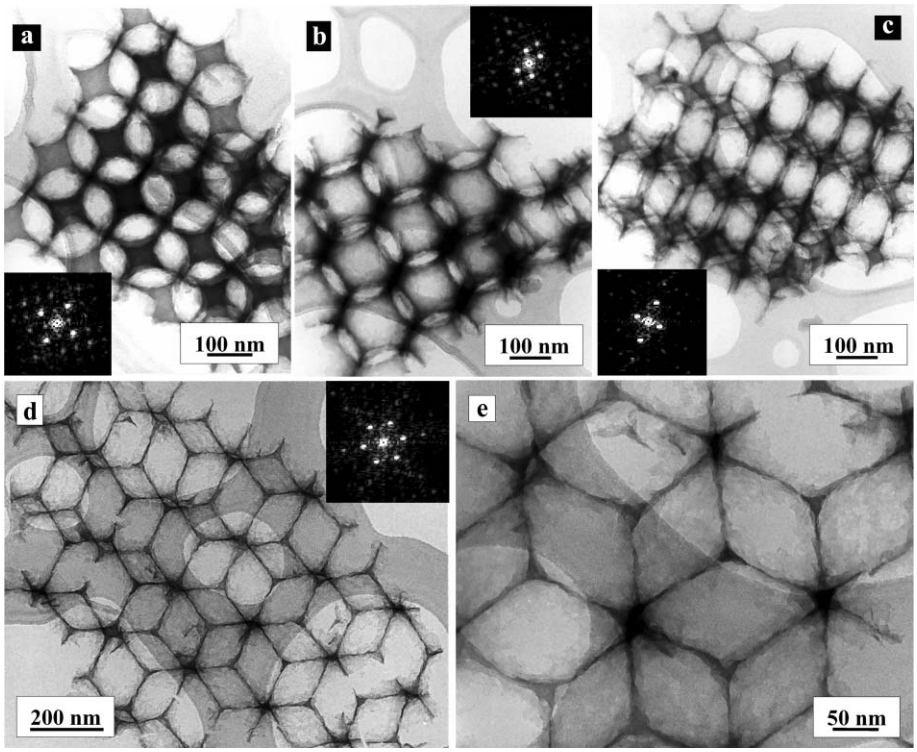

Fig. 5 TEM images of amorphous silica imprinted on PS-HEMA. The porous structure is projected along the [100] (a), [110] (b), [211] (c) and [111] (d,e) directions.

silicate precursors, the low viscosity of the solution assists the infusion process and when suction is applied, a liquid film is retained in the free spaces inside the template by capillary forces. Under the pH and concentration conditions used in the experiments, $Si(OH)_4$ is the predominant species in the solution. The monomers polymerize to form particles that grow and link with each other throughout the solution to produce a gel. As a result of the low gelation rate a homogeneous thin layer is formed between the microspheres and this fact accounts for the film wall structure and poor thickness observed in porous silica. Similar wall structure and thickness have been reported for ordered macroporous alumina obtained by hydrolysis of aluminium tri-*sec*-butoxide with butan-2-ol as solvent.[12] However, macroporous titania obtained from titanium isopropoxide diluted in *n*-propanol or hexane and templated by PS-HEMA microspheres shows greater wall thickness than silica together with smaller pore diameter and greater contraction of the structure. These results can be discussed bearing in mind the different reactivity of silica and titania precursors and also the fact that the chemical properties

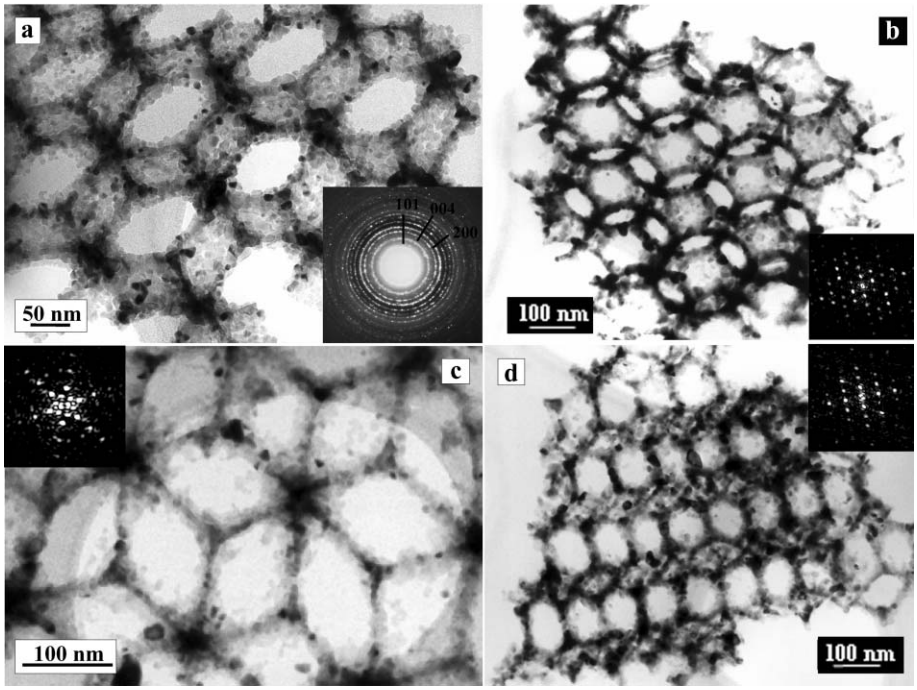

Fig. 6 Macroporous titania obtained from titanium isopropoxide–*n*-propanol using PS-HEMA as template and treated at 500 °C for 3 hours. The micrographs show the pore walls formed of anatase nanocrystals (a), and the projections of the structure along the directions close to [110] (b), [111] (c) and [211] (d).

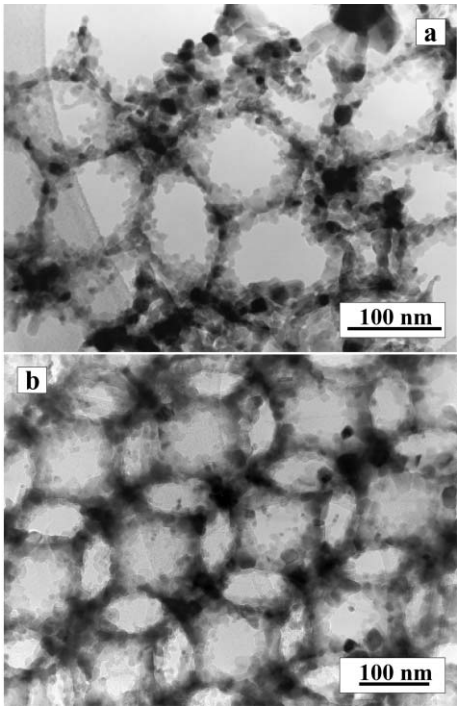

Fig. 7 Macroporous titania obtained from titanium isopropoxide–hexane using PS-HEMA as templated and treated at 500 °C for 3 hours. The porous structure is projected along the [111] (a) and [110] (b).

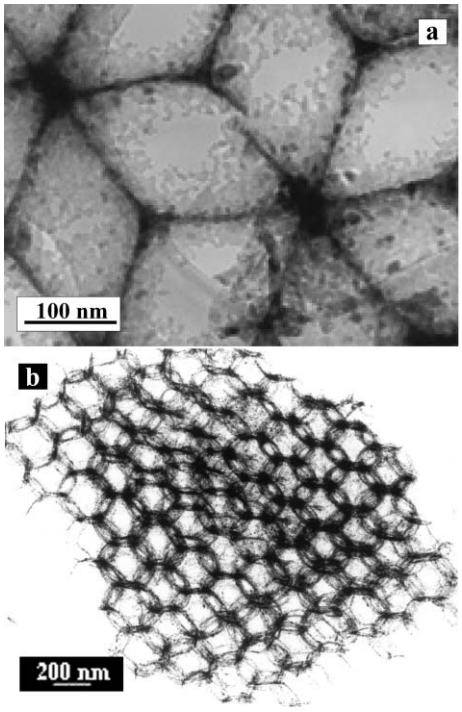

Fig. 8 Macroporous titania imprinted on PS microspheres and treated at 500 °C for 3 hours. The images correspond to the projections along [111] (a) and close to [110] (b) directions.

of the latex particles can affect the hydrolysis and condensation processes. Compared with silicon, transition metals have lower electronegativities and can exhibit several coordination states. Therefore, the transition metal alkoxides show high reactivity with donor groups. Alkoxy bridging and nucleophilic addition of solvent molecules as well as water allow the metal atoms to expand their coordination. Therefore, the complexity of the precursor and the hydrolysis and condensation rates are determined by the nature of the alkoxide and the solvent.[30] Titanium isopropoxide is monomeric since the steric effects of the alkoxy groups prevent the formation of alkoxy bridges. When the alkoxide is diluted in *n*-propanol or hexane, solvent molecules can be coordinated due to the tendency of the metal to expand its coordination, but the formation of metal–solvate bonds occurs with alcohol molecules rather than with an inert solvent. In both cases, hydrolysis and condensation are fast processes and the products are polydisperse powders.[30] However, hydrolysis and condensation processes inside the latex arrays could be affected by the fact that donor groups at the surface of the particles can be involved in nucleophilic attack on the metal atoms. The carboxylic groups of the HEMA chains can compete with the solvent molecules and the metal alkoxide monomers could be retained at the surface of the latex particles. This process must be more important when the full coordination of the metal atoms is not already satisfied, as is the case with titanium isopropoxide in hexane. It is known that when acetic acid is added to monomeric titanium isopropoxide the coordination number of the titanium increases from 4 to 6 and IR and EXAFS results[31] show that bridging and terminal alkoxide ligands and bridging carboxylate ligands are present. Chelating ligands have also been used in the synthesis of mesostructured titania from titanium isopropoxide with surfactant molecules as templates.[32] The structure-directing effect of the surfactant is improved because the reaction with the chelating agent lowers the reactivity of the titania precursor. In a similar way carboxylic groups of the HEMA chains, which retain titanium alkoxide monomers, can promote the formation of polymer over the surface of the particles when bridging alkoxide and carboxylate ligands are formed. During hydrolysis the alkoxide groups are preferentially hydrolysed whereas carboxylate ligands remain bonded to titanium and as far as the condensation pathway is concerned, the wall microstructure and thickness can also be affected. To investigate the influence of the chemistry at the particle-monomer interface on the microstructural parameters, PS latex particles have also been used to template porous titania.

Macroporous titania imprinted on PS microspheres. PS latex particles used to template porous titania were assembled by filtration and the cavities between the microspheres were mineralized by capillarity with titanium isopropoxide diluted in *n*-propanol (weight ratio alkoxide : alcohol $\approx$ 0.6). For this sample (Fig. 8), the mean pore diameter ranges from 290 to 310 nm and the estimated contraction of the structure is about 20%. The pore wall is made of anatase nanocrystals. The thickness ranges from 6 to 8 nm and the pore windows are partially covered with thin crystallites, most of them with major dimensions ranging from 6 to 10 nm. The pore wall thickness is thinner than that obtained when titania is templated by PS-HEMA particles. However, titania templated by PS and silica show some resemblance (compare micrographs Figs. 5e and 8a). In these samples the microstructure of the pore wall is different because of the amorphous character of silica but in both cases the wall thickness and structural shrinkage are very similar. These results seem to indicate that chemical interactions do not occur between the precursors and the latex particles in either silica or titania templated by PS latex. Therefore, the latex composition seems to affect the microstructural parameters. Pore wall microstructure, crystallite size and thickness depend on the nature of the precursor and solvent but, they must also depend on the particle surface–precursor interactions.

Our results also seem to indicate that as far as the infiltration route is concerned, a high degree of filling with the precursor solution can be achieved using both filtration and capillary forces methods. The lack of order, observed in some particles, is due to disordered regions in the template when it has been obtained by deposition. However, infiltration by capillarity

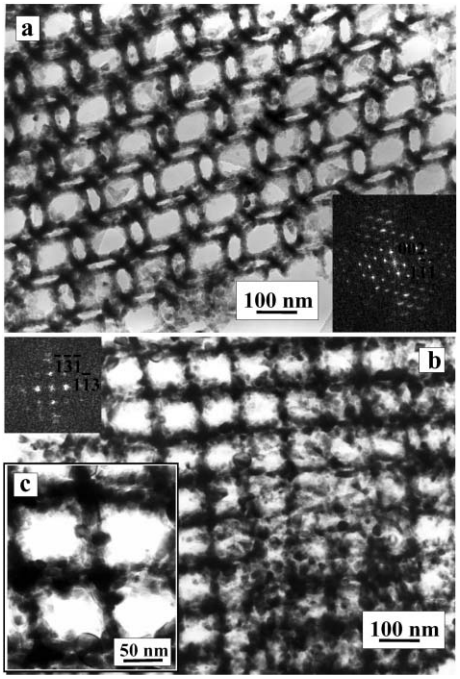

Fig. 9 Macroporous titania imprinted on PS-HEMA and treated at 550 °C (a) and 600 °C (b) for 16 hours. The images correspond to projections along the [110] (a) and [$\bar{5}$12] (b) directions.

seems to be a suitable procedure to avoid an excess of precursor above the template film.

Effect of the thermal treatment on macroporous titania. A portion of titania taken from the sample treated at 500 °C (shown in Fig. 6) was also treated at 550 °C and 600 °C for 16 hours at each temperature. No significant changes are found when the sample is treated at 550 °C and most of the particles show a well ordered porous structure (Fig. 9a). This structure is also preserved after treatment at 600 °C but the growth of the crystals produces windows that are partially closed and in some particles disordered areas appear (Fig. 9b).

Conclusions

PS-HEMA and PS monodisperse spherical particles form highly ordered arrays when the solvent is removed by either evaporation of the solvent in air at room temperature or by filtration. During evaporation of the water, attractive capillary forces and convective flux help the particles organize themselves in close packed structures. In the latex arrangements prepared by this method the degree of order and the efficiency of packing is higher than in the case of the arrays obtained by filtration processes where kinetic and steric factors and cooperative effects must control nucleation and growth of the arrays.

Mineralization of the cavities in the latex structures produces networks of three-dimensionally interconnected pores into the skeleton of the ceramics. Amorphous silica and anatase nanocrystals form, in each case, the pore wall in the macroporous skeleton. In porous titania the pore wall thickness, crystallite size and structural shrinkage are affected by interactions that occur between the titania precursor and donor groups at the surface of the latex particles. Therefore, the latex composition seems to be important in order to control the microstucture parameters of the imprinted porous solids.

Acknowledgements

The authors are grateful to UCM for financial support under a multidisciplinary project. We also thank A. Rodríguez and Centro de Microscopía Electrónica at UCM for technical assistance. Dr M. Martínez and Dr R. Serrano are acknowledged for helping in the synthesis of latex samples. We also acknowledge Dr F. Ortega for collaboration in LS characterization of the latex suspensions and Dr J. A. Campos for obtaining the UV/Vis spectra. E. Enciso also thanks Dr A. Ureña for the use of laboratory equipment. E. Enciso and M. C Carbajo acknowledge Project n° PB 98/0673-C02-02 of MCT (Spain).

References

1 J. Liu, X. Feng, G. E. Fryxell, L. Q. Wang, A. Y. Kim and M. Gong, *Adv. Mater.*, 1998, **10**(2), 161.
2 Y. Wei, L. M. Fan, S. X. Jiang, B. H. Yang and L. R. Chen, *Anal. Lett.*, 1998, **31**(9), 1487.
3 M. Müller, R. Zentel, T. Maka, S. G. Romanov and C. M. Sotomayor Torres, *Adv. Mater.*, 2000, **12**(20), 1499.
4 N. Raman, M. T. Anderson and C. J. Brinker, *Chem. Mater.*, 1996, **8**, 1682.
5 B. T. Holland, C. F. Blanford and A. Stein, *Science*, 1998, **281**, 538.
6 O. D. Velev and A. M. Lenhoff, *Curr. Opin. Colloid Interf. Sci.*, 2000, **5**, 56.
7 M. J. Kim and R. Ryoo, *Chem. Mater.*, 1999, **11**, 487.
8 A. Imhof and D. J. Pine, *Nature*, 1997, **389**, 948.
9 V. N. Manoharan, A. Imhof, J. D. Thorne and D. J. Pine, *Adv. Mater.*, 2001, **13**, 447.
10 O. D. Velev, T. A. Jede, R. F. Lobo and A. M. Lenhoff, *Nature*, 1997, **389**, 448.
11 A. A. Zakhidov, R. H. Baughman, Z. Iqbal, C. Cul, I. Khayrullin, S. O. Dantas, J. Marti and V. G. Ralchenko, *Science*, 1998, **282**, 897.
12 B. T. Holland, C. F. Blanford, T. Do and A. Stein, *Chem. Mater.*, 1999, **11**, 795.
13 M. E. Turner, T. J. Trentler and V. L. Colvin, *Adv. Mater.*, 2001, **13**(3), 180.
14 O. D. Velev, T. A. Jede, R. F. Lobo and A. M. Lenhoff, *Chem. Mater.*, 1998, **10**, 3597.
15 B. Gates, Y. Yin and Y. Xia, *Chem. Mater.*, 1999, **11**, 2827.
16 Q. Luo, A. Liu, L. Li, S. Xie, J. Kong and D. Zhao, *Adv. Mater.*, 2001, **13**(4), 286.
17 D. Wang, R. A. Caruso and F. Caruso, *Chem. Mater.*, 2001, **13**, 364.
18 S. A. Johnson, P. J. Ollivier and T. E. Mallouk, *Science*, 1999, **283**, 963.
19 J. L. Keddie, *Mater. Sci. Eng.*, 1997, **21**, 101.
20 H. Du, P. Chen, F. Liu, F. Mentg, T. Lli and X. Tnag, *Mater. Chem. Phys.*, 1997, **51**, 227.
21 Y. Xia, B. Gates, Y. Yin and Y. Lu, *Adv. Mater.*, 2000, **12**(10), 693.
22 O. D. Velev and E. W. Kaler, *Adv. Mater.*, 2000, **12**(7), 531.
23 A. H. Cardoso, C. A. P. Leite, M. E. Darbello Zaniquelli and F. Galembeck, *Colloid Surf. A*, 1998, **144**, 207.
24 J. W. Goodwin, R. H. Ottewill, R. Pelton, G. Vianello and D. E. Yates, *Br. Polym. J.*, 1978, **10**, 173.
25 S. Rakers, L. F. Chi and H. Fuchs, *Langmuir*, 1997, **13**, 7121.
26 N. D. Denkov, O. D. Velev, P. A. Kralchevsky, I. B. Ivanov, H. Yoshimura and K. Nagayama, *Langmuir*, 1992, **8**, 3183.
27 N. D. Denkov, O. D. Velev, P. A. Kralchevsky and I. B. Ivanov, *Nature*, 1993, **361**, 26.
28 J. Rieger, E. Hädicke, G. Ley and P. Lindner, *Phys. Rev. Lett.*, 1992, **68**(18), 2782.
29 S. Jons, P. Ries and C. J. McDonald, *J. Membr. Sci.*, 1999, **155**, 79.
30 J. Livage, M. Henry and C. Sanchez, *Prog. Solid State Chem.*, 1988, **18**(4), 259.
31 J. Livage, C. Sanchez, M. Henry and S. Doenff, *Solid State Ionics*, 1989, **32**(33), 633.
32 M. Fröba, O. Muth and A. Reller, *Solid State Ionics*, 1997, **101–103**, 249.